

Theoretical study of 1D gradient photonic structures with quartic polynomial dielectric profile formed by $\text{Al}_l\text{Ga}_{1-l}\text{As}$ varying pressure and temperature under oblique incidence

D.M. Calvo-Velasco^{a,b,*}, Robert Sánchez-Cano^a

^a Departamento de Física, Universidad Autónoma de Occidente, 2790, Cali, Colombia

^b Departamento de Ciencias Básicas, Corporación Universitaria Comfacauca, 190001, Santander de Quilichao, Colombia

ARTICLE INFO

Keywords:

Gradient profile
Photonic system
Analytic solution
Graphene
Pressure and temperature dependence

ABSTRACT

In this work it is presented a theoretical study of the optical properties of 1D photonic systems with gradient dielectric profile layers of quartic polynomial type, using the dielectric $\text{Al}_l\text{Ga}_{1-l}\text{As}$ being the Al concentration along the width of the slab as the gradient function, when external parameters as the pressure and the temperature are considered. It is shown that the proposed gradient profile admits an analytic approach supported on the method of series to find the solutions of the wave equations for the TE and TM polarizations. Also, it is proposed a new regression model for the calculation of the dielectric value of $\text{Al}_l\text{Ga}_{1-l}\text{As}$ as a function of the pressure and temperature. The results showed that the increase in the pressure shifts and changes the transmission bands due to the decrease in the dielectric mean value of the gradient slab. On the other hand, it is found that the increase in the temperature shifts the transmission bands to lower frequencies but without changing their shape distribution. Considering the inclusion of graphene, it is observed its effect on the distribution of the transmission bands at different frequencies depending on the graphene properties. It is expected that the proposed structure can contribute to the development of new devices when the pressure, the temperature and the chemical potential of graphene are used as external tunable parameters.

1. Introduction

In the last decades the study of 1D photonic systems with periodic spatial dielectric functions in one dimension have attracted great interest since their unique abilities to control electromagnetic waves thanks to the formation of photonic band gaps, this is frequency bands for which the propagation of electromagnetic radiation is forbidden [1–3]. It is known that band gaps depend on the distribution of the material which form the photonic structure [4,5], but also they could be modulated thanks to external agents which vary the optical properties of the constitutive materials [6]. In this way, doped semiconductors under external magnetic fields have been considered thanks to the modulation of the electromagnetic force on the semiconductor free charges by the magnetic field [7,8]. It has been demonstrated that the inclusion of graphene in this structures leads to the formation of absorption multi-channels that can be tuned, which could be used in the construction of optical devices as polarization sensors and photo-detectors [9–11]. On the other hand, the inclusion of superconductors allows to

have optical systems that vary their properties not only with the distribution of the constituents materials but with the external temperature, due to the change in the superconductor properties above or below their characteristic critical temperature, affecting their transmission band distribution which can be tuned to different frequency values [12–17]. In a similar way, the effect of the external pressure on the photonic structures allows to control their optical properties due to the modification of the geometric material distribution [18,19]. These external and geometric parametric variations are used to guided the construction of different optical devices which are proposed as sensor for: biomarkers, salinity, glucose among other, thanks to their long durability and usability in comparing with sensors based on chemical processes [20–23].

On the other hand, in recent years the study of photonic systems based in gradient profiles of the refractive index have been widely explore, due to their emergent optical properties which are not reached by the use of homogeneous dielectric materials [24–30]. In the case of 1D photonic gradient structures, the general theoretical approach

* Corresponding author. Departamento de Ciencias Básicas, Corporación Universitaria Comfacauca, 190001 Santander de Quilichao, Colombia.

E-mail address: dannycalvo@unicomfacauca.edu.co (D.M. Calvo-Velasco).

<https://doi.org/10.1016/j.cap.2022.06.008>

Received 2 March 2022; Received in revised form 26 May 2022; Accepted 12 June 2022

Available online 23 June 2022

1567-1739/© 2022 Korean Physical Society. Published by Elsevier B.V. All rights reserved.

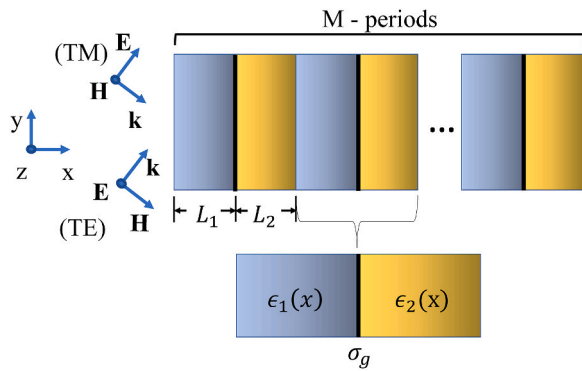


Fig. 1. Schematic representation of the 1D photonic structure constructed with M periods of alternating slabs with gradient index profile material $\epsilon_1(x)$ and $\epsilon_2(x)$ respectively, with sheets of graphene represented by its conductivity σ_g . The transverse electric (TE) and transverse magnetic (TM) polarizations are represented.

limited these studies to normal incidence, due to the implicit difficult in exploring exact analytical solutions for the electromagnetic fields under oblique incidence. These studies are typically limited to profiles as linear, exponential or logarithmic for which solutions in terms of functions of Bessel can be found.

In the case of oblique incidence, the solutions are based on the long wavelength approach, in which each gradient material layer is simulated as a set of homogeneous dielectric layers, which are thin in comparison with the incident radiation wavelength [31]. The problem with this method is that it must be considered a large number of partitions with the increases of the frequency value. This approach suggests in the limit case of a large number of layers the gradient profile is reached.

According to our investigation, the polynomial gradient profile of the dielectric function has not been considered, in addition there is not including their variation due to external agents like pressure and temperature, for that reason, in this work it is studied a system formed by layers of material with a gradient dielectric profile of quartic polynomial type, considering the variation of external parameters of pressure and temperature [18,32–34]. Unlike other works in which the analytical solutions are limited the case of normal incidence, in this work it is presented that for this type of dielectric profile is possible to raise solutions, for the functions that describe the radiation distribution of the electromagnetic field in the layers, in form of series considering oblique incidence. They are applied to the case of dielectric $\text{Al}_l\text{Ga}_{1-l}\text{As}$, where the profile variation is related to the concentration of Al_l in the layer. For the numerical calculations, the transfer matrix method is used [35], and the different dielectric properties for each one of the considered profiles are described as function of the pressure and the temperature. In this study is proposed a new regression model for the dielectric value of $\text{Al}_l\text{Ga}_{1-l}\text{As}$ as function of the considered external agents. This work is distributed as follow: first it presented the analytic approach for the transfer matrix formalism, then it explored the form of the solutions for the proposed dielectric profile, next, the description of the gradient profiles and the dependence of the dielectric value for the chosen material is presented. Finally, the results and the conclusion of this work are also given.

2. Theoretical framework

Considering the system presented in Fig. 1, formed by two slabs of material with gradient dielectric function separated by graphene layer, it is possible to show that the wave equation that describes the behavior of the electric field in each of the slab materials for the TE polarization, $\vec{E} = (0, 0, E_z)$, has the form

$$\partial_x^2 E_z + (k_0^2 \epsilon(x) - k_y^2) E_z = 0. \quad (1)$$

being $k_0 = \omega/c$, $k_y = k_0 \sin(\varphi)$, φ the incidence angle and $\epsilon(x)$ the dielectric function with gradient profile. In a similar way, for the TM polarization, $\vec{H} = (0, 0, H_z)$ the wave equation has the form

$$\partial_x^2 H_z - \frac{\epsilon'(x)}{\epsilon(x)} \partial_x H_z + (k_0^2 \epsilon(x) - k_y^2) H_z = 0. \quad (2)$$

As it is observed the differential equations are of order two and for an arbitrary dielectric profile their have as solutions two linear independent functions, so that the general solutions can be expressed as a linear combination of them [36]. It is important to mention that in the case of the TM polarization eq. (2), the convergence ratio for the solutions of eq. (2) depend on the zeros of $\epsilon(x)$. Next, it is explore the transfer matrix formalism for the proposed structure.

2.1. Transference matrix formalism considering graphene

Consider the system presented in Fig. 1, formed by M periods of bilayers of materials with gradient index profile described by the dielectric functions as $\epsilon_1(x)$ and $\epsilon_2(x)$ which are separated by a graphene sheet, with a surface conductivity calculated in Refs. [37,38] and described by

$$\sigma_g = \sigma_g^{intra} + \sigma_g^{inter}, \quad (3)$$

$$\sigma_g^{intra} = \frac{e^2}{4\hbar} \frac{i}{2\pi} \left(\frac{16k_B T}{\hbar\omega} \ln \left(2 \cosh \left(\frac{\mu_g}{2k_B T} \right) \right) \right), \quad (4)$$

$$\sigma_g^{inter} = \frac{e^2}{4\hbar} \left(\frac{1}{2} + \frac{1}{\pi} \arctan \frac{\hbar\omega - 2\mu_g}{2k_B T} - \frac{i}{2\pi} \ln \frac{(\hbar\omega + 2\mu_g)^2}{(\hbar\omega - 2\mu_g)^2 + (2k_B T)^2} \right), \quad (5)$$

where e is the electron charge, k_B is the Boltzmann constant, T is the temperature (in Kelvin degrees) and μ_g is the chemical potential of the graphene sheets, which can be modified by the gate voltages.

Taking into account the isotropy of the materials and by using the wave propagation equations for the TE and TM polarizations, equations (1) and (2) respectively, the propagation of the z -component of the electric (magnetic) field, for TE (TM) polarization, in each of the gradient slabs, can be written as

$$F_z^j(x) = A_j f_j(x) + B_j g_j(x), \quad (6)$$

with f_j and g_j two independent solutions of equations (1) and (2) which can be chosen to satisfied the initial conditions [24]

$$\begin{bmatrix} f_j(0) & g_j(0) \\ f_j'(0) & g_j'(0) \end{bmatrix} = \begin{bmatrix} 1 & 0 \\ 0 & 1 \end{bmatrix}. \quad (7)$$

The amplitudes of the fields at the different interfaces are related through the transfer matrix defined by [39]

$$\begin{bmatrix} A_j \\ B_j \end{bmatrix} = M_{jj-1} \begin{bmatrix} A_{j-1} \\ B_{j-1} \end{bmatrix}, \quad (8)$$

with M_{jj-1} the transfer matrix at the interface of the slab j and $j - 1$, either for TE or TM polarization, which are constructed by applying the boundary conditions of the fields at the material interfaces. Due to the surface conductivity of the graphene sheets between the gradient slabs a surface current is presented, modifying the continuity of the magnetic field at the interface in the form of [40]

$$\vec{n}_{j,j+1} \times \left(\vec{H}_{j+1} - \vec{H}_j \right) = \sigma_g \vec{E}_t, \quad (9)$$

being $\vec{n}_{j,j+1}$ the normal vector at the interface between the j and $j + 1$ slab, and \vec{E}_t the tangential component of the electric field at the surface.

Under this condition the transference matrix for the proposed system can be written as

$$M_T = (M_2^P [I + G] M_1^P)^M, \tag{10}$$

with I the identity matrix of order two, M_j^P the material matrix which depend on $\epsilon_j(x)$ and the polarization P , and

$$G = g \begin{bmatrix} -1 & -(+)1 \\ +(-)1 & 1 \end{bmatrix} \tag{11}$$

with $g = k_0 \sigma_g Z_0 / 2Q_0$ ($g = \sigma_g Z_0 Q_0 / 2k_0$), for TE (TM) polarization, and Z_0 the impedance of empty space and $Q_0 = k_0 \cos \varphi$. It is possible to find that

$$M_j^{TE} = A^{-1} S_j^{TE} (L_j) A, \tag{12}$$

$$M_j^{TM} = \frac{\epsilon_j(0)}{\epsilon_j(L_j)} B_j^{-1} (L_j) S_j^{TM} (L_j) B_j(0), \tag{13}$$

where

$$S_j^P(x) = \begin{bmatrix} f_j(x) & g_j(x) \\ f_j'(x) & g_j'(x) \end{bmatrix}, \tag{14}$$

is a matrix constructed with the two independent solutions for 1 and 2, for the TE and TM polarization respectively, and

$$A = \begin{bmatrix} 1 & 1 \\ iQ_0 & -iQ_0 \end{bmatrix}, \tag{15}$$

$$B_j(x) = \begin{bmatrix} 1/\epsilon_j(x) & 1/\epsilon_j(x) \\ iQ_0 & -iQ_0 \end{bmatrix}. \tag{16}$$

The inclusion of graphene in between the dielectric materials allows to improve the control of the optical properties of the proposed structure thanks to the change of the graphene chemical potential through the application of a gate voltage on it [41–43].

2.2. Dielectric profiles and series solutions

In this work, the considered dielectric profiles are quartic polynomials, this is

$$\epsilon(x) = Ax^4 + Bx^3 + Cx^2 + Dx + E, \tag{17}$$

under this function, it is possible to describe the solutions of equations (1) and (2) as series of x

$$F(x) = \sum_{n=0}^{\infty} c_n x^n, \tag{18}$$

which in case of the TE polarization goes to the recurrence relations for the c_n coefficients as

$$c_{n+2} = \frac{-(k_0^2 E - k_y^2) c_n - k_0^2 (Dc_{n-1} + Cc_{n-2} + Bc_{n-3} + Ac_{n-4})}{(n+2)(n+1)}, \tag{19}$$

and for the TM polarization

$$\begin{aligned} c_{n+2} = & \left(D(1 - n^2) c_{n+1} + (Cn(3 - n) - E(k_0^2 E - k_y^2)) c_n \right. \\ & + (B(n - 1)(5 - n) - D(2k_0^2 E - k_y^2)) c_{n-1} \\ & + (A(n - 2)(7 - n) - (k_0^2 \gamma - Ck_y^2)) c_{n-2} \\ & - (k_0^2 \delta - Bk_y^2) c_{n-3} - (k_0^2 \gamma - Ak_y^2) c_{n-4} - k_0^2 \beta c_{n-5} \\ & \left. - k_0^2 \alpha c_{n-6} - 2k_0^2 ABC c_{n-7} - k_0^2 A^2 c_{n-8} \right) / (n+2)(n+1) E, \end{aligned} \tag{20}$$

with $\alpha = 2AC + B^2$, $\beta = 2AD + 2BC$, $\gamma = 2AE + 2BD + C^2$, $\delta = 2BE + 2CD$, and $\chi = 2CE + D^2$. As it was mention, the convergence ratio of the solutions depend on the zeros of $\epsilon(x)$, especially the TM polarization, and

also on the frequency value. On the other hand, for an computational approach the series needs to take and upper bound, in the presented work this limits reach the 400 therms in its expansion.

2.3. Gradient slab profile description

The studied systems are made with slabs of gradient dielectric profile considering the dielectric properties of the material $\text{Al}_l\text{Ga}_{1-l}\text{As}$, being l the Al concentration. In order to model the dielectric response of the gradient slab as a function of pressure and temperature it was used a similar approach to that presented in Ref. [18], where was fitted the experimental results presented in Ref. [44] for the GaAs material using the model

$$\epsilon_{\text{GaAs}}(P, T) = (\epsilon_0 + (AT + BT^2)e^{\alpha(T)T})e^{\beta(T)P}, \tag{21}$$

with $\epsilon_0 = 12.677717$, $A = 5.461388 \times 10^{-4} \text{ K}^{-1}$, $B = 3.418165 \times 10^{-6} \text{ K}^{-2}$, and where $\alpha(T)$ and $\beta(T)$ are linear extrapolation functions of the temperature with the porpoise of consider the exponential dependence for the dielectric permittivity presented in the Table II of [44]. The dependence of these functions are

$$\alpha(T) = (5 / 102)T + (484 / 85), \tag{22}$$

in 10^{-5} K^{-1}

$$\beta(T) = (-1 / 374)T - 16.48786. \tag{23}$$

in $10^{-4} \text{ kbar}^{-1}$. This model can be considered valid in the range of $T < 400\text{K}$, and $P < 40 \text{ kbar}$.

On the other hand, the dielectric permittivity of the $\text{Al}_l\text{Ga}_{1-l}\text{As}$ is modeled using the proposed of [45,46] through the function

$$\epsilon_{\text{AlGaAs}}(l, P, V) = \epsilon_{\text{GaAs}}(P, V) - 3.12l. \tag{24}$$

Meanwhile, the effect of the pressure on the variation of the thickness of the slabs of $\text{Al}_l\text{Ga}_{1-l}\text{As}$ its modeled through the model of [47]

$$d(l, P) = d_0 [1 - (S_{11}(l) + 2S_{12}(l))P], \tag{25}$$

where the elastic constants present a dependence with the Al concentration, as

$$\begin{aligned} S_{11}(l) &= 1.17 + 0.03l \\ S_{12}(l) &= -0.37 - 0.02l \end{aligned} \tag{26}$$

in $10^{-3} \text{ kbar}^{-1}$.

In this work the gradient profile is modeled as a function of the shape concentration of Al, this means as a function of $l(x)$ which depends on the slab thickness x . Due to this dependence, the shape profile is modified by the pressure and the temperature, and to assure the convergence of the proposed solutions it is necessary to study the behavior of the $\epsilon(x)$ and its variations as functions of the pressure and the temperature.

In order to present a systematic way to study these variations, it is necessary to propose a gradient profile for given pressure and temperature, (P_0, T_0), then using the variations of the width of the gradient slab, the modifications of the gradient profile can be determined.

Is it easy to demonstrated that if $l(x, P_0)$ is chosen for (P_0, T_0), the slab width presents an effective variation as

$$d = d_0 [1 - \alpha P], \tag{27}$$

with d_0 the initial slab thickness and

$$\begin{aligned} \alpha &= \frac{1}{d_0} \int_0^{d_0} [S_{11}(l(x, P_0)) + 2S_{12}(l(x, P_0))] dx \\ &= 0.43 - \frac{0.01}{d_0} \int_0^{d_0} l(x) dx \end{aligned} \tag{28}$$

Table 1

Description of the parameter values of the dielectric gradient profile $\epsilon(x, P_0, T_0) = Ax^4 + Bx^3 + Cx^2 + Dx + E$ for $P_0 = 0$ kbar and $T = 0K$.

Profile	A	B	C	D	E
1	0	0	3.12	0	9.5577171
2	0	0	-3.12	0	12.6777171
3	0	9.21585	-4.42712	-4.65842	12.5474

in 10^{-3} kbar $^{-1}$. In the same way the concentration profile for and arbitrary pressure is described as

$$l(x, P) = l(x/d, P_0). \tag{29}$$

As it is observed, the concentration profile is rescaled, as a function of the pressure. In this case the gradient dielectric function is

$$\epsilon(x, P, T) = \epsilon_{GaAs}(P, V) - 3.12l(x, P). \tag{30}$$

3. Results

The studied photonic systems are constructed by 20 bilayers of air and a material with gradient dielectric profile constructed with the dielectric Al₁Ga_{1-l}As, considering a graphene sheet in between. The different profiles are described in Table 1, which were chosen to ensure the convergence of the solutions in the study bandwidth from 0 to 8 THz, for the values of $P = 0$ kbar and $T = 0K$. In order to satisfy the quarter wave approximation in the case of $l = 0$, when the central frequency is 3 THz, the width of the air layer is 25 μ m and for the gradient layer of 7 μ m given a length for the structure of 640 μ m. On this work, the effect on the air layer parameters due to pressure and temperature are negligible, and the effect of losses in the dielectric layers are not considered.

In Fig. 2 it is presented the effect on the transmittance diagram due to the pressure. It is observed that the increase in the pressure allows to shift the transmission bands to higher frequencies, result in accordance to Refs. [18,32], but also with the changing in their shapes. This is due to the decrease in the dielectric mean value of the gradient slab, which also presents the decrease in their width [48]. These two effects decrease the bandwidth of the first band gap, but also contributed to the increase of the region with low transmission observed at higher frequencies. In comparing the TE and TM transmission diagrams is observed an omnidirectional band gap only for the TE polarization, limited at below for a transmission band with low dispersion even for high incident angles, and at above by a band with a high dispersion. In this case the modification of the band distribution with the pressure, varies the functionality of this system as a polarization selective sensor with variable bandwidth, as example for an incidence angle of 45 in (a) it is observed a transmission band centered around the 5 THz with a bandwidth of approximated 1 THz with high transmission for the TM mode, in contrast in (c) the center frequency is shifted at around 5.4 THz with a bandwidth of approximated 0.8THz. On the other hand in Fig. 3, the increase in the temperature influence the shifting of the transmission band at lower frequencies, this is due to the increase in the dielectric effective value of the gradient slab. In this case it is not observed the changing in the transmission bands shapes, in a different way to the pressure effect, because the slab width does not depend on the temperature. As it was found, the pressure effect on the transmittance is more evident in comparing to the temperature effect.

This allows to propose that the gradient slab profile has more interesting variations to that observed on systems with homogeneous dielectric slabs, due to the changing in the transmission band shape or in the shifting of their central frequencies at lower or higher frequencies with the variations of the pressure or the temperature. These results

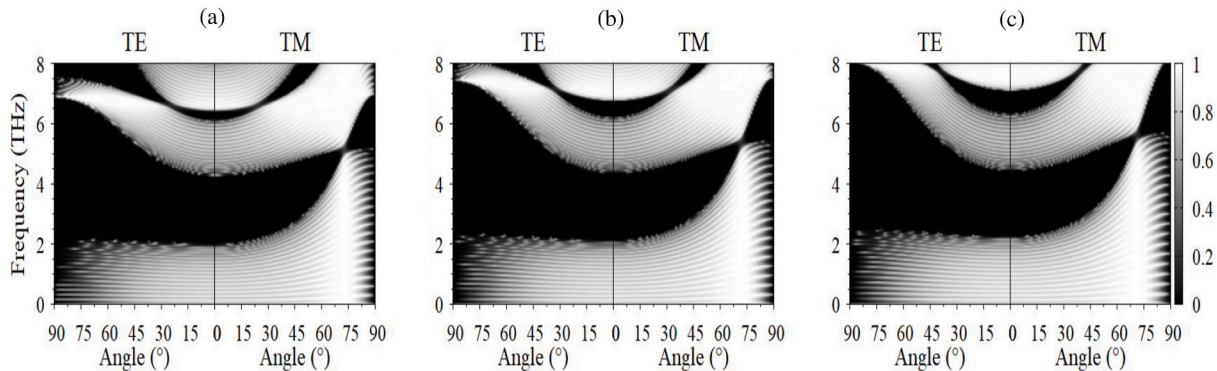


Fig. 2. Transmission diagrams for TE and TM polarizations considering the profile 1 described in Table 1, considering the variation of pressure ($T = 0K$): (a) $P = 0$ kbar, (b) $P = 50$ kbar, and (c) $P = 100$ kbar, without graphene layers.

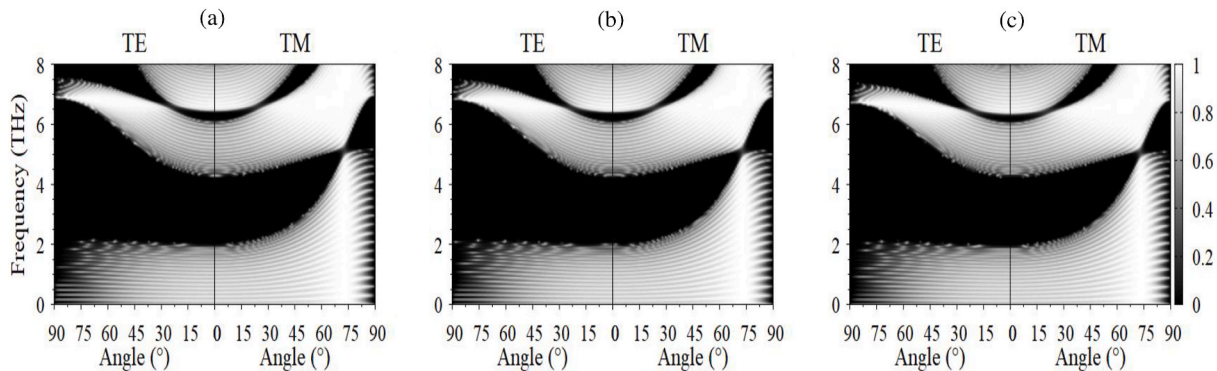


Fig. 3. Transmission diagrams for TE and TM polarizations considering the profile 1 described in Table 1, considering the variation of temperature ($P = 0$ kbar): (a) $T = 0K$, (b) $T = 150K$, and (c) $T = 300K$, without graphene layers.

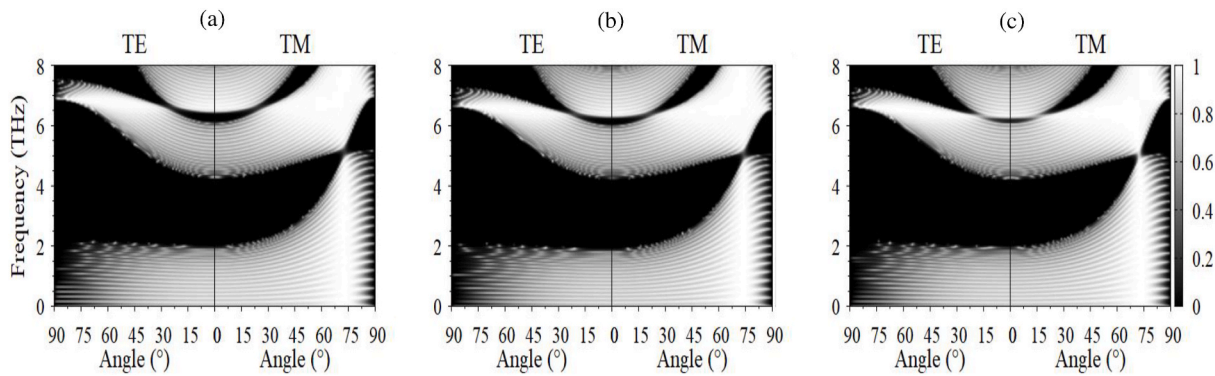


Fig. 4. Transmission diagrams for TE and TM polarizations considering the different profiles described in Table 1 for $P = 0$ kbar and $T = 0$ K: (a)Profile 1, (b)Profile 2, and (c)Profile 3, without graphene layers.

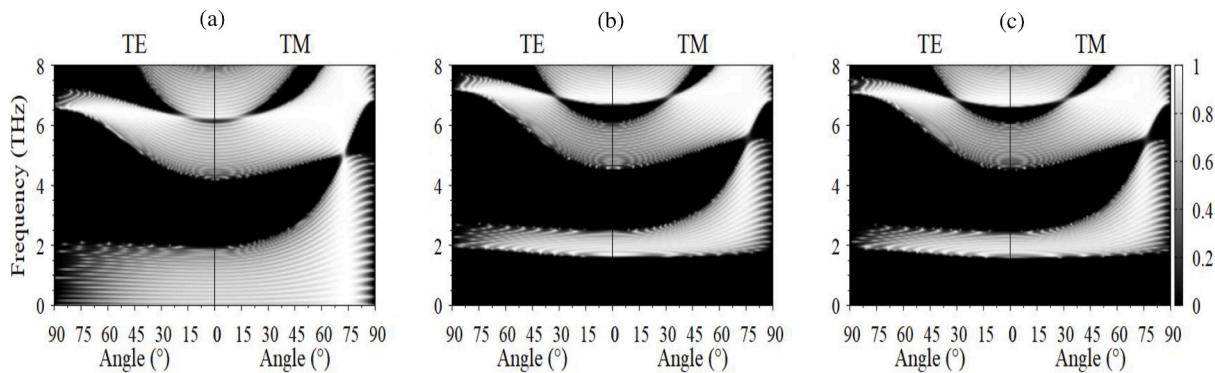


Fig. 5. Transmission diagrams for TE and TM polarizations considering the profile 3 described in Table 1, for $P = 0$ kbar when: (a) $T = 150$ K without graphene, (b) $T = 150$ K with graphene, and (c) $T = 300$ K with graphene.

were also observed for the other profiles, which are not presented here. On the other hand, it was observed the redistribution of the transmission bands depending on the profile shape, as is presented in Fig. 4. In this case, the main effect is due to the dielectric effective mean value of the gradient slab. In comparing, the dielectric mean value for the profile 2 is higher to that for the profile 1, for that reason the transmission bands in (b) are located at lower frequencies to that observed in (a). Meanwhile, the effect due to shape profile, is observed in (c), in this situation the profiles 2 and 3 have similar effective dielectric mean values, but in their transmittance diagrams are notice, for example the transmission low regions at higher frequencies. Finally, it is presented the effect in the transmission when there are inserted graphene layers. As is presented in Fig. 5 the inclusion of graphene layers, induce the formation of an omnidirectional band gap at low frequencies, this result it was observed in other studies [41–43], but also is observed the grow of the low transmission regions at higher frequencies for the proposed dielectric profile. On the other hand, the increase in the temperature shift the transmission band gaps a lower frequencies, also decreasing the first bandgap width. As it was found in other studies, the variations on the graphene properties varies the transmission diagram, especially the chemical potential of graphene, which can be tuned for the application of a gate voltage on the graphene layers. This property promotes the studied structure to be a candidate to open a route to design optoelectronic devices when the pressure, the temperature, and the chemical potential of graphene are used as external tunable parameters [49].

4. Conclusions

As conclusions, in this work it was presented the optical properties of systems with gradient dielectric profile of polynomial type when external parameters as the pressure and temperature are considered. It

was proposed an analytic approach to the solutions of the wave equation for the TE and TM polarizations using the method of series, also implementing their in the transfer matrix method in order to calculate the transmittance. The considered dielectric material to construct the gradient profile was $\text{Al}_x\text{Ga}_{1-x}\text{As}$ using as gradient function the aluminium concentration along the width of the slab. For this dielectric it was proposed a new expression for the calculation of their dielectric permittivity value as a function of the pressure and temperature, using a regression model where the parameters related with the exponential dependence of the permittivity vary linearly with the temperature. Also, it was proposed a methodology to explore the properties of the gradient slab in term of the gradient Al concentration profile. It was found that the increase in the pressure shifts and changes the transmission bands to higher frequencies due to the decrease in the dielectric mean value of the gradient slab and the decrease in the slab width. On the other hand, the increase of the temperature shifts the transmission bands to lower frequencies but without changing the shape distribution, due to the increase of the dielectric effective mean value of the slab. Considering the inclusion of graphene, it was found the formation of a band gap at low frequencies also with the shifting of the transmission band gaps due to the variation of the temperature. It is expected that these results contributed to the development of new devices when the pressure, the temperature and the chemical potential of graphene are used as external tunable parameters.

Declaration of competing interest

The authors declare that they have no known competing financial interests or personal relationships that could have appeared to influence the work reported in this paper.

Acknowledgement

Authors thank to Dr. Feng Wu from the School of Optoelectronic Engineering, Guangdong Polytechnic Normal University, for useful comments and critical reading of the manuscript. Also, authors wants to thanks to the Colombian Scientific Ministry Minciencias by its financial support (Grant No. 848-2019) and to the Universidad Autónoma de Occidente where part of this study was made.

References

- [1] Y. Fink, J.N. Winn, S. Fan, C. Chen, J. Michel, J.D. Joannopoulos, E.L. Thomas, A dielectric omnidirectional reflector, *Science* 282 (5394) (1998) 1679–1682.
- [2] F. Wu, K. Lyu, S. Hu, M. Yao, S. Xiao, Ultra-large omnidirectional photonic band gaps in one-dimensional ternary photonic crystals composed of plasma, dielectric and hyperbolic metamaterial, *Opt. Mater.* 111 (2021), 110680.
- [3] F. Wu, X. Wu, S. Xiao, G. Liu, H. Li, Broadband wide-angle multilayer absorber based on a broadband omnidirectional optical tamm state, *Opt Express* 29 (Jul 2021) 23976–23987.
- [4] A.H. Aly, Metallic and superconducting photonic crystal, *J. Supercond. Nov. Magnetism* 21 (2008) 421.
- [5] A.H. Aly, C. Malek, H.A. Elsayed, Transmittance properties of a quasi-periodic one-dimensional photonic crystals that incorporate nanocomposite material, *Int. J. Mod. Phys. B* 32 (21) (2018), 1850220.
- [6] Y. Trabelsi, W. Belhadj, N. Ben Ali, A.H. Aly, Theoretical study of tunable optical resonators in periodic and quasiperiodic one-dimensional photonic structures incorporating a nematic liquid crystal, *Photonics* 8 (5) (2021).
- [7] N. Chittaranjan, S. Ardhendu, A. Alireza, Periodic multilayer magnetized cold plasma containing a doped semiconductor, *Indian J. Phys.* 92 (2018) 911–917.
- [8] Chittaranjan Nayak, Alireza Aghajamali, Dipak P. Patil, Extrinsic magnetized plasma fabry-perot resonator, *Indian J. Phys.* 93 (2019) 401–406.
- [9] A. Rashidi, C. Nayak, C.G. Bezerra, C.H. Costa, F.A. Pinheiro, Tunable terahertz absorption in Si/SiO₂-graphene multilayers: disorder and magneto-optical effects, *Appl. Opt.* 59 (Dec 2020) 11034–11040.
- [10] A. Padhy, R. Bandyopadhyay, C.H. Costa, C.G. Bezerra, C. Nayak, Enhanced transmission induced by embedded graphene in periodic, quasiperiodic, and random photonic crystals, *J. Opt. Soc. Am. B* 37 (Dec 2020) 3801–3808.
- [11] N. Chittaranjan, S. Ardhendu, A. Alireza, Enhanced transmission induced by embedded graphene in periodic, quasiperiodic, and random photonic crystals, *J. Opt. Soc. Am. B* 37 (Dec 2020) 3801–3808.
- [12] A.H. Aly, H.-T. Hsu, T.-J. Yang, C.-J. Wu, C.K. Hwangbo, Extraordinary optical properties of a superconducting periodic multilayer in near-zero-permittivity operation range, *J. Appl. Phys.* 105 (8) (2009), 083917.
- [13] A.H. Aly, D. Mohamed, The optical properties of metamaterial-superconductor photonic band gap with/without defect layer, *J. Supercond. Nov. Magnetism* 32 (2019) 1897–1902.
- [14] W. Sabra, A.H. Aly, A comparative study of the effective surface impedance of an HTc superconducting thin film from visible to mid-IR region, *Opt. Quant. Electron.* 53 (2021) 416.
- [15] A.H. Aly, S.E.-S. Abdel Ghany, B.M. Kamal, D. Vigneswaran, Theoretical studies of hybrid multifunctional YBa₂Cu₃O₇ photonic crystals within visible and infra-red regions, *Ceram. Int.* 46 (1) (2020) 365–369.
- [16] A.H. Aly, Doaa Mohamed, M.A. Mohaseb, Metamaterial control of hybrid multifunctional high-*tc* superconducting photonic crystals for 1D quasi-periodic structure potential applications, *Mater. Res.* 23 (2020), e20190695.
- [17] Y. Trabelsi, N.B. Ali, A.H. Aly, M. Kanzari, Tunable high *tc* superconducting photonic band gap resonators based on hybrid quasi-periodic multilayered stacks, *Physica C: Superconductivity and its Applications* 576 (2020), 1353706.
- [18] N. Porras-Montenegro, C. Duque, Temperature and hydrostatic pressure effects on the photonic band structure of a 2D honeycomb lattice, *Phys. E Low-dimens. Syst. Nanostruct.* 42 (6) (2010) 1865–1869.
- [19] A.H. Aly, F.A. Sayed, THz cutoff frequency and multifunction Ti₂Ba₂Ca₂Cu₃O₁₀/GaAs photonic bandgap materials, *Int. J. Mod. Phys. B* 34 (10) (2020), 2050091.
- [20] I.S. Amiri, B.K. Paul, K. Ahmed, A.H. Aly, R. Zakaria, P. Yupapin, D. Vigneswaran, Tri-core photonic crystal fiber based refractive index dual sensor for salinity and temperature detection, *Microw. Opt. Technol. Lett.* 61 (3) (2019) 847–852.
- [21] A. Natesa, K.P. Govindasamy, T.R. Gopal, V. Dhasarathan, A.H. Aly, Tricore photonic crystal fibre based refractive index sensor for glucose detection, *IET Optoelectron.* 13 (3) (2019) 118–123.
- [22] Z.A. Zaky, A.M. Ahmed, A.S. Shalaby, A.H. Aly, Refractive index gas sensor based on the Tamm state in a one-dimensional photonic crystal: Theoretical optimisation, *Sci. Rep.* 10 (2020) 9736.
- [23] S.R. Qutb, A.H. Aly, W. Sabra, Salinity and temperature detection for seawater based on a 1D-defective photonic crystal material, *Int. J. Mod. Phys. B* 35 (1) (2021), 2150012.
- [24] G.V. Morozov, D.W.L. Sprung, J. Martorell, One-dimensional photonic crystals with a sawtooth refractive index: another exactly solvable potential, *New J. Phys.* 15 (oct 2013), 103009.
- [25] B.K. Singh, P. Kumar, P.C. Pandey, Tunable photonic band-gaps in one-dimensional photonic crystals containing linear graded index material, *Appl. Phys. B* 117 (3) (2014) 947–956.
- [26] B.K. Singh, M.K. Chaudhari, P.C. Pandey, Photonic and omnidirectional band gap engineering in one-dimensional photonic crystals consisting of linearly graded index material, *J. Lightwave Technol.* 34 (10) (2016) 2431–2438.
- [27] A.H. Gevorgyan, Nonreciprocity of waves in 1D photonic quasiperiodic crystals, *J. Contemp. Phys.* 42 (2007) 139–144.
- [28] A.J. Hussein, Z.M. Nassar, S.A. Taya, Dispersion properties of slab waveguides with a linear graded-index film and a nonlinear substrate 27, *Microsystem Technologies*, 2021, pp. 2589–2594.
- [29] B. Xu, G. Zheng, Y. Wu, K. Cao, Transmission properties of defect modes in one-dimensional photonic crystals containing gradient refractive index defects, *Optik* 126 (24) (2015) 5158–5162.
- [30] C.-Y. Liu, Flexible photonic nanojet formed by cylindrical graded-index lens, *Crystals* 9 (4) (2019).
- [31] S. Roshan Entezar, Optical bistability in one-dimensional photonic band gap structure with nonlinear graded-index defect layer, *Opt Commun.* 287 (2013) 19–24.
- [32] L.E. González, N. Porras-Montenegro, Pressure, temperature and plasma frequency effects on the band structure of a 1D semiconductor photonic crystal, *Phys. E Low-dimens. Syst. Nanostruct.* 44 (4) (2012) 773–777.
- [33] F. Segovia-Chaves, H. Vinck-Posada, E. Navarro-Barón, TE band structure in a photonic waveguide with triangular holes, *Optik* 200 (2020), 163436.
- [34] F. Segovia-Chaves, E.N. Barón, H. Vinck-Posada, Photonic band structure in a one-dimensional distributed Bragg reflector pillar, *Mater. Res. Express* 7 (2020) 126201.
- [35] P. Yeh, A. Yariv, C.-S. Hong, Electromagnetic propagation in periodic stratified media. I. General theory, *J. Opt. Soc. Am.* 67 (Apr 1977) 423–438.
- [36] C.H. Edwards, D.E. Penney, *Elementary Differential Equations*, Pearson Prentice Hall, 2008.
- [37] L.A. Falkovsky, A.A. Varlamov, Space-time dispersion of graphene conductivity, *Eur. Phys. J. B* 56 (4) (2007) 281–284.
- [38] L.A. Falkovsky, S.S. Pershoguba, Optical far-infrared properties of a graphene monolayer and multilayer, *Phys. Rev. B* 76 (Oct 2007) 153410.
- [39] A. Bruno-Alfonso, E. Reyes-Gómez, S.B. Cavalcanti, L.E. Oliveira, Unfolding of plasmon-polariton modes in one-dimensional layered systems containing anisotropic left-handed materials, *Phys. Rev. B* 84 (Sep 2011) 113101.
- [40] D. Calvo-Velasco, N. Porras-Montenegro, Tunable optical response at the plasmon-polariton frequency in dielectric-graphene-metamaterial systems, *Superlattice. Microst.* 116 (2018) 244–252.
- [41] A. Madani, S.R. Entezar, Optical properties of one-dimensional photonic crystals containing graphene sheets, *Phys. B Condens. Matter* 431 (2013) 1–5.
- [42] L. Zhang, G. Wang, X. Han, Y. Zhao, Transmission property of one-dimensional multilayer graphene-dielectric stack, *Optik - Int. J. Light Electron Optic.* 127 (4) (2016) 2030–2035.
- [43] F. Wu, M. Chen, Z. Chen, C. Yin, Omnidirectional terahertz photonic band gap broaden effect in one-dimensional photonic crystal containing few-layer graphene, *Opt Commun.* 490 (2021), 126898.
- [44] G.A. Samara, Temperature and pressure dependences of the dielectric constants of semiconductors, *Phys. Rev. B* 27 (Mar 1983) 3494–3505.
- [45] S. Adachi, GaAs, AlAs, and Al_xGa_{1-x}As: material parameters for use in research and device applications, *J. Appl. Phys.* 58 (3) (1985) R1–R29.
- [46] A. Sivakami, V. Gayathri, Hydrostatic pressure and temperature dependence of dielectric mismatch effect on the impurity binding energy in a spherical quantum dot, *Superlattice. Microst.* 58 (2013) 218–227.
- [47] A.M. Elabasy, Hydrostatic pressure dependence of binding energies for donors in quantum well heterostructures, *Phys. Scripta* 48 (sep 1993) 376–378.
- [48] D. Calvo-Velasco, R. Sánchez-Cano, Omnidirectional photonic band gaps in one-dimensional gradient refractive index photonic crystals considering linear and quadratic profiles, *Curr. Appl. Phys.* 35 (2022) 72–77.
- [49] Z.A. Zaky, A.H. Aly, Modeling of a biosensor using Tamm resonance excited by graphene, *Appl. Opt.* 60 (Feb 2021) 1411–1419.